p-type behavior from Sb-doped ZnO heterojunction photodiodes

L. J. Mandalapu, F. X. Xiu, Z. Yang, D. T. Zhao, and J. L. Liu[a)]
Quantum Structures Laboratory, Department of Electrical Engineering, University of California, Riverside, California 92521

(Received 15 September 2005; accepted 31 January 2006; published online 15 March 2006)

Antimony (Sb) doping was used to realize *p*-type ZnO films on *n*-Si (100) substrates by molecular beam epitaxy. These samples were fabricated into *p*-*n* heterojunction diodes. *p*-type behavior of Sb-doped ZnO was studied by carrying out *I*-*V* and capacitance-voltage (*C*-*V*) measurements. *I*-*V* curves showed rectifying behavior similar to a *p*-type Schottky diode with a turn-on voltage around 2.4 V, which is consistent with the Schottky barrier of about 2.2 V obtained from *C*-*V* characterization. Good photoresponse in the UV region was obtained, which further proved that Sb doping could be used to fabricate *p*-type ZnO for photodetector and other optoelectronic applications. © *2006 American Institute of Physics*. [DOI: 10.1063/1.2186516]

ZnO has attracted significant attention in the last few years for its potential optoelectronic applications in the UV region, such as photodetectors and light-emitting diodes, etc., because of its suitable band gap (~3.3 eV) and large exciton binding energy (~60 meV).[1,2] However, it is difficult to achieve high-quality *p*-type ZnO material due to the possibility of holes getting compensated by the "intrinsic" donors such as zinc interstitials (Zn_i) and oxygen vacancies (V_o).[3,4] To obtain *p*-type ZnO, group V elements such as N,[5] P,[6] and As[7] have been tried experimentally as dopants. A few ZnO heterojunctions employing N-doped *p*-ZnO on *n*-Si,[8] P-doped *p*-ZnO on *n*-GaN,[9] and Al–N-codoped- *p*-ZnO on *n*-Si (Ref. 10) and also limited homojunctions[11–13] have been reported. However, good device performances are yet to be demonstrated. Recently, based on first-principle calculations it was predicted that another group V element Sb could introduce shallow acceptor levels in ZnO, assuming that an Sb atom would substitute a Zn atom and simultaneously produce two Zn vacancies.[14] Consistent with this theory, Sb-doped ZnO films were grown by molecular beam epitaxy (MBE) in our group, and Hall effect measurements indeed showed strong *p*-type conduction for these films.[15] In this letter, we report *p*-type behavior of Sb-doped ZnO films based on Sb-doped *p*-ZnO/*n*-Si heterojunction device structures. The optical detection performances of these devices are also demonstrated.

ZnO thin films were grown on *n*-Si (100) substrates of resistivity 20–30 Ω cm using an electron-cyclotron-resonance (ECR)-assisted Perkin-Elmer MBE system. Zn and Sb sources were provided by effusion cells with solid Zn (5N) and Sb (6N) shots. Oxygen source was from pure O_2 (5N) gas and oxygen plasma was generated using an ECR tube. The Si substrates were cleaned with $H_2O_2+H_2SO_4$ (3:5) and diluted HF solutions alternately three times, and then dried with nitrogen gas. The substrates were also thermocleaned under vacuum at 650 °C for 10 min prior to growth. The Sb-doped ZnO layer was grown at 550 °C using an Sb cell temperature of 350 °C. The samples were annealed *in situ* at 650 °C for 30 min to activate the dopants. The thickness of the resultant ZnO layer is around 200 nm.

Standard photolithography techniques were employed to fabricate the samples into *p*-*n* diodes. Al/Ti (250 nm/20 nm) metal contact pads of 120 μm × 180 μm were deposited on the Sb-doped ZnO layer using electron-beam evaporation and lift-off technology. Al/Ti metal of 250 nm/20 nm was also deposited on the backside of the Si substrate to form the second electrode of the *p*-*n* diode. A pair of contacts was made on the backside of a separate piece of the sample to check for Ohmic contact formation. The contacts were annealed at 550 °C for 30 s. Figures 1(a) and 1(b) shows the *I*-*V* characteristics on log-log scale for a pair of contacts as-deposited and after annealing on *p*-ZnO, respectively. The measurements were carried out using an Agilent 4155C semiconductor parameter analyzer. The characteristics from the as-deposited contacts show the presence of a barrier close to 1 V. A double-Schottky behavior can be observed from the inset of Fig. 1(a) which shows both the forward and reverse *I*-*V* characteristics on a linear scale. The magnitude of current conducted by them is also very small leading to a very high contact resistance in the order of megaohms. Annealing the contacts at 550 °C for 30 s resulted in establishment of Ohmic contacts. The linear characteristics of current over more than two orders of magnitude from the annealed contacts on ZnO layer show Ohmic conduction and absence of any barriers. The bottom-right inset in Fig. 1(b) shows both the forward and reverse characteristics on a linear scale. Transmission line method measurements were used to estimate the contact and sheet resistances of contacts annealed at 550 °C. The resistance measured between electrodes with different spacing is plotted as the top-left inset of Fig. 1(b). The contact and sheet resistances are calculated to be about 5.1 kΩ and 674 Ω/sq, respectively. The contact resistance can be lowered to about 600 Ω by annealing further at 750 °C, but the contact morphology degrades severely. Hence, a compromise at the cost of high contact resistance was made. The contact on Si layer was also ensured to be Ohmic. The current conducted by the contacts on ZnO layer was found to be smaller than that on the Si layer by an order of magnitude due to the possible reason of relatively higher contact resistance from ZnO contacts, thin film thickness and low mobility of holes.

Hall effect and resistivity measurements were carried out on the sample at room temperature with van der Pauw configuration. The hole concentration, mobility, and resistivity

[a)]Author to whom correspondence should be addressed; electronic mail: jianlin@ee.ucr.edu

 © 2006 American Institute of Physics
Downloaded 16 Mar 2006 to 138.23.166.8. Redistribution subject to AIP license or copyright, see http://apl.aip.org/apl/copyright.jsp

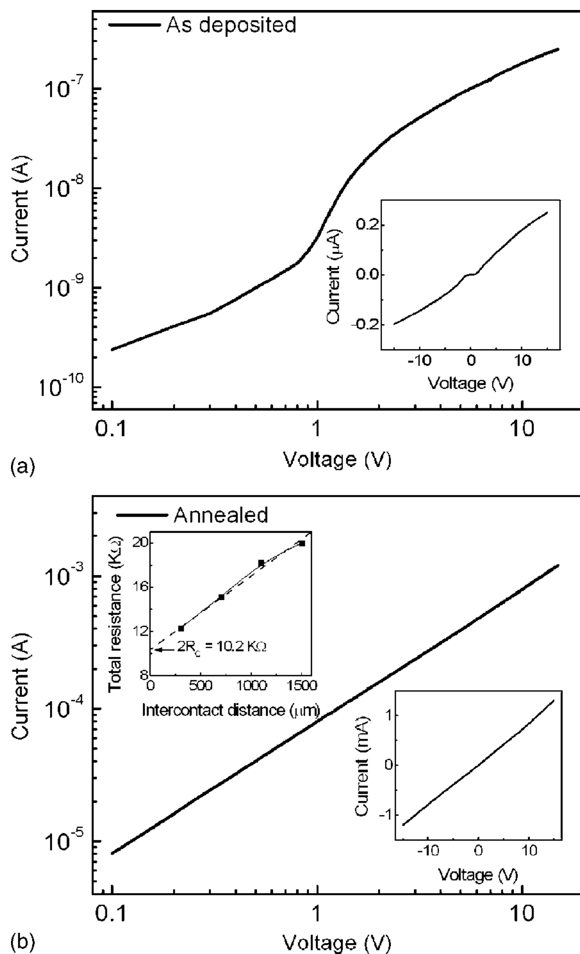

FIG. 1. *I-V* curves of (a) as-deposited and (b) annealed contacts on ZnO, respectively. Right-bottom insets show the corresponding forward and reverse characteristics on a linear scale. The top-left inset in (b) shows the total resistance between the annealed contacts as a function of contact spacing.

of the Sb-doped ZnO layer are 1.0×10^{18} cm^{-3}, 22.4 cm^2 V^{-1} S^{-1}, and 0.27 Ω cm, respectively. Photoluminescence (PL) characterization of the sample was performed at 8.5 K. The PL spectrum was excited by a 325 nm He–Cd laser and detected by a photomultiplier tube. The Sb-related acceptor bound exciton emission was observed at 3.356 eV, which is in good agreement with our previous study[15] and the acceptor binding energy of Sb is estimated to be 0.2 eV.

Figure 2 shows the *I-V* characteristics of the heterojunction diode plotted on a semilogarithmic scale. Clear rectifying curves for the device were observed but the rectification has an inverse trend of a *p-n* junction as clearly seen from the linear-scale plot in the inset on left. Since Ohmic contacts were established on both the ZnO and Si layers, we conclude the nonlinear behavior to appear from the ZnO–Si junction. This suggests that the diode is a *p*-type Schottky diode. The turn-on voltage of the diode is around −2.4 V as seen from the *I-V* curves. The right inset in Fig. 2 shows the energy band diagram of the heterojunction at equilibrium. The energy band diagram was constructed based on Anderson's model,[16,17] by using the electron affinity of Si ($\chi_{Si}=4.05$ eV) (Ref. 17) and ZnO ($\chi_{ZnO}=4.35$ eV).[18] The left side region represents *p*-type ZnO with Sb doping and the right side is *n*-type Si substrate. Because the ZnO layer was heavily doped with a hole concentration of 1.0×10^{18} cm^{-3}, the Fermi level in ZnO should be very close

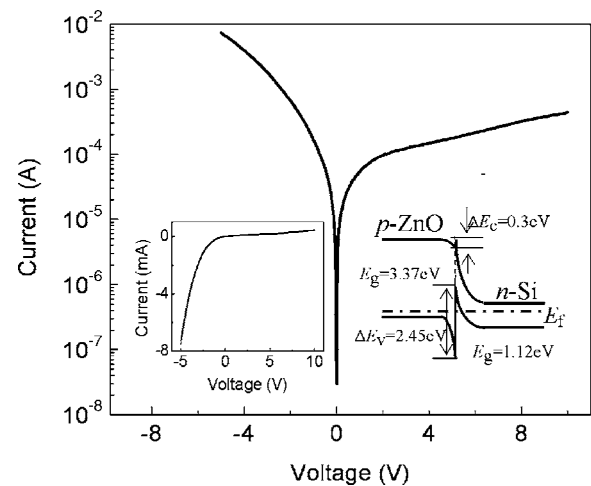

FIG. 2. *I-V* characteristics of the *p*-ZnO/*n*-Si photodiode in dark. Rectifying characteristics similar to that of a *p*-type Schottky diode is observed. The right inset shows the energy band diagram of the heterojunction at equilibrium. Inset on the left shows the *I-V* curves on a linear scale.

to its valence band edge. The band diagram shows a small conduction band offset of 0.3 eV and a large valence band offset of 2.45 eV, respectively. At the equilibrium, a quantum well for holes is formed on the Si side at the interface. The valence band offset acts as a barrier for the conduction of holes from *p*-ZnO to *n*-Si, thus limiting the conducted current. Here, the smaller band gap Si is comparable to the metal and the valence band offset is equivalent to a Schottky barrier in a *p*-type diode. The forward *I-V* characteristics follow the relation for the thermionic emission over a barrier: $J_F=A^*T^2\exp(-e\Phi_b/kT)\exp(eV/nkT)$, where, J_F is the current density, A^* is the Richardson's constant for *p*-ZnO, T is the absolute temperature, e is the electronic charge, Φ_b is the barrier height, k is the Boltzmann's constant, n is the ideality factor, and V is the applied voltage. Nevertheless, the ideality factor was not determined because the precise area of the junction is not known, as mesas were not defined in this experiment. The dark current is large, about 1.76×10^{-4} A at 5 V due to the imperfect ZnO/Si interface and poor heteroepitaxial ZnO film quality. The diode did not show any signs of breakdown even if the bias reaches 40 V, although there was an increase in the leakage current.

Capacitance-voltage (*C-V*) measurements at a frequency of 100 kHz were made using an Agilent 4284A precision LCR meter. Typical characteristics of the *p*-type Schottky diode again were observed as shown in Fig. 3. High forward bias was avoided during the measurements as large forward bias current and diffusion capacitance may affect the accuracy of the capacitance measurement. The inset of the Fig. 3 shows the linear $1/C^2$-*V* curve. The Schottky barrier height is estimated to be about 2.2 V by extrapolating the curve in the reverse bias region. This value is in good agreement with the turn-on voltage obtained from *I-V* measurements. The slope of the $1/C^2$-*V* curve changes in the forward bias region, which may arise from the interface states due to the poor quality of heteroepitaxy.

Figure 4 shows the voltage dependent photocurrent (PC) spectra as a function of wavelength obtained from the heterojunction photodiode that was diced and packaged on a TO5 can. The PC measurements were carried out using a 150 W Xe arc lamp and a 1/4 m monochromator. A chopper was used to chop light before casting it on the device. The

Downloaded 16 Mar 2006 to 138.23.166.8. Redistribution subject to AIP license or copyright, see http://apl.aip.org/apl/copyright.jsp

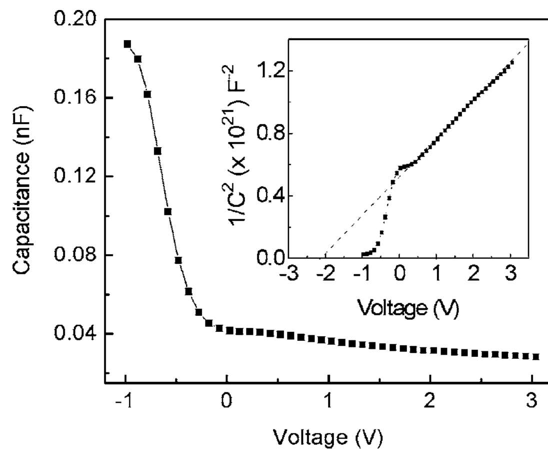

FIG. 3. *C-V* curve of the heterojunction device measured in dark. The inset gives the $1/C^2$-*V* characteristics of the photodiode. The Schottky barrier is estimated by extrapolating the linear region of the $1/C^2$-*V* curve.

generated PC was amplified by a homebuilt preamplifier and fed to the lock-in amplifier. The incident power on the device was calibrated using a commercial UV enhanced Si photodiode, from which the responsivity values were obtained. As seen from Fig. 4, detection can be observed in the UV region as well as the visible region. Most of the UV response can be attributed to the absorption in wide band gap ZnO layer as the high-energy UV light is absorbed by ZnO before it reaches the Si layer. Additionally, the high-energy light is limited by its penetration depth in ZnO. Peak absorption in UV region is around 350 nm (corresponding to the effective band gap of ZnO, 3.54 eV) due to the presence of high density of states. Increase in the response starting from wavelengths beyond approximately 368 nm, which corresponds to the band gap of ZnO, can be seen. This is because, once the energy of the incident photons is smaller than the band gap of ZnO, ZnO becomes transparent to such light and the quantum well region at the interface and the wide depletion region in Si start the absorption. The depletion region extends deeper into the *n*-Si side due to its low dopant concentration compared to the *p*-type ZnO layer, because of which the response in visible region is higher. The small peaks in the PC curves at the wavelengths of 398 and 470 nm are from the UV source lines and can be neglected. The response increases with increase in the reverse (positive) bias as shown in Fig. 4. The PC signal dies when a negative bias is applied to ZnO side, which again confirms the Schottky diode structure. In the photovoltaic mode of operation, responsivities of about 0.0958 and 1.73 A/W are obtained for 353 and 400 nm light, respectively.

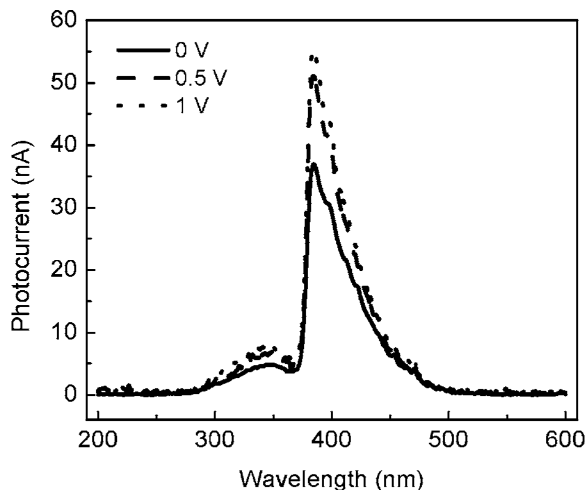

FIG. 4. PC spectra of the device under reverse bias voltages of 0, 0.5, and 1 V.

In summary, Sb-doped *p*-type ZnO films grown by MBE were studied by fabricating them into heterojunction device structures. Device characteristics such as the rectifying *I-V* curves and the *C-V* curves show typical *p*-type Schottky diode behavior, which arises from wide band gap *p*-type ZnO on narrow band gap *n*-type Si. The diodes exhibit a turn-on voltage of 2.4 V, which is consistent with the *C-V* measurements. The diodes also have a good photoresponse in both the UV region and visible region. Responsivity of about 95.8 mA/W for 353 nm UV light at no bias was observed. The demonstration of these first Sb-doped *p*-type ZnO/*n*-type Si heterojunction diodes suggests that Sb is a promising element for *p*-type doping in ZnO for UV optoelectronic applications.

The authors acknowledge the financial support from DARPA/DMEA through the UCR Center for Nanoscience and Innovation for Defense (CNID) under Award No. H94003-04-2-0404.

[1] D. C. Look, Mater. Sci. Eng., B **B80**, 383 (2001).
[2] S. J. Pearton, D. P. Norton, K. Ip, and Y. W. Heo, J. Vac. Sci. Technol. B **22**, 932 (2004).
[3] D. C. Look, J. W. Hemsky, and J. R. Rizelove, Phys. Rev. Lett. **82**, 2552 (1999).
[4] S. B. Zhang, S. H. Wei, and A. Zunger, Phys. Rev. B **63**, 075205 (2001).
[5] D. C. Look, D. C. Reynolds, C. W. Litton, R. L. Jones, D. B. Eason, and G. Cantwell, Appl. Phys. Lett. **81**, 1830 (2002).
[6] K. K. Kim, H. S. Kim, D. K. Hwang, J. H. Lim, and S. J. Park, Appl. Phys. Lett. **83**, 63 (2003).
[7] Y. R. Ryu, S. Zhu, D. C. Look, J. M. Wrobel, H. M. Jeong, and H. W. White, J. Cryst. Growth **216**, 330 (2000).
[8] D. Wang, Y. C. Liu, R. Mu, J. Y. Zhang, Y. M. Lu, D. Z. Shen, and X. W. Fan, J. Phys.: Condens. Matter **16**, 4635 (2004).
[9] D. K. Hwang, S. H. Kang, J. H. Lim, E. J. Yang, J. Y. Oh, J. H. Yang, and S. J. Park, Appl. Phys. Lett. **86**, 222101 (2005).
[10] F. Zhuge, L. P. Zhu, Z. Z. Ye, D. W. Ma, J. G. Lu, J. Y. Huang, F. Z. Wang, Z. G. Ji, and S. B. Zhang, Appl. Phys. Lett. **87**, 092103 (2005).
[11] A. Tsukazaki, A. Ohtomo, T. Onuma, M. Ohtani, T. Makino, M. Sumiya, K. Ohtani, S. F. Chichibu, S. Fuke, Y. Segawa, H. Ohno, H. Koinuma, and M. Kawasaki, Nat. Mater. **4**, 42 (2005).
[12] T. Aoki, Y. Hatanaka, and D. C. Look, Appl. Phys. Lett. **76**, 3257 (2000).
[13] Y. R. Ryu, W. J. Kim, and H. W. White, J. Cryst. Growth **219**, 419 (2000).
[14] S. Limpijumnong, S. B. Zhang, S. H. Wei, and C. H. Park, Phys. Rev. Lett. **92**, 155504 (2004).
[15] F. X. Xiu, Z. Yang, L. J. Mandalapu, D. T. Zhao, J. L. Liu, and W. P. Beyermann, Appl. Phys. Lett. **87**, 152101 (2005).
[16] R. L. Anderson, Solid-State Electron. **5**, 341 (1962).
[17] S. M. Sze, *Physics of Semiconductor Devices*, 2nd ed. (Wiley, New York, 1981).
[18] J. A. Aranovich, D. G. Golmayo, A. L. Fahrenbruch, and R. H. Bube, J. Appl. Phys. **51**, 4260 (1980).

Downloaded 16 Mar 2006 to 138.23.166.8. Redistribution subject to AIP license or copyright, see http://apl.aip.org/apl/copyright.jsp